Supplement of Atmos. Chem. Phys., 22, 1195–1208, 2022
https://doi.org/10.5194/acp-22-1195-2022-supplement

Atmospheric Chemistry and Physics
Open Access
EGU

Supplement of

Comparison of saturation vapor pressures of α-pinene + O_3 oxidation products derived from COSMO-RS computations and thermal desorption experiments

Noora Hyttinen et al.

Correspondence to: Noora Hyttinen (noora.x.hyttinen@jyu.fi)

Table S1: Temperatures of maximum desorption with 20 s averaging (in K) and experimental saturation vapor pressures[a] of the calibration compounds (PEG6, PEG7 and PEG8).

Compound	run 1	run 2	run 3	p_{sat} (Pa)[a]
$C_{12}H_{26}O_7$	316.82	316.80	317.32	3.05×10^{-5}
$C_{14}H_{30}O_8$	337.99	336.87	337.52	1.29×10^{-6}
$C_{16}H_{34}O_9$	352.07	349.29	356.85	9.20×10^{-8}

[a] The experimental saturation vapor pressures were taken from Krieger et al. [S1]

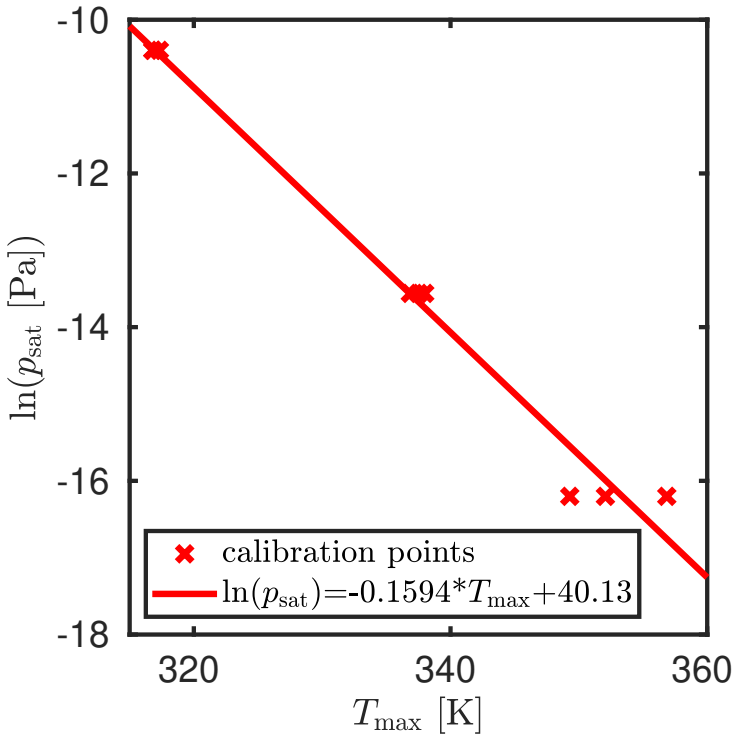

Figure S1: Calibration of the 20 s averaged thermograms at 298.15 K. The compounds used in the calibration are polyethylene glycols (PEG) $C_{12}H_{26}O_7$, $C_{14}H_{30}O_8$ and $C_{16}H_{34}O_9$ (PEG6, PEG7 and PEG8, respectively). The values used in the calibration are shown in Table S1.

Table S2: Difference in T_{max} between linear (lin) and polynomial (pol) calibration fit in Ylisirniö et al.,[a] linear calibration fit of this study. The estimate for the polynomial fit for calibration data from this study was calculated by subtracting the ΔT_{max} from the linear calibration fit.

p_{sat} (Pa)	$T^{a}_{max,pol}$ (K)	$T^{a}_{max,lin}$ (K)	ΔT_{max} (K)	$T^{b}_{max,lin}$ (K)	$T^{b}_{max,pol}$ (K)
3.6×10^{-5}	306	305	-1	316	317
1.6×10^{-6}	324	323	-1	335	337
9.0×10^{-8}	339	340	1	354	353
3.9×10^{-9}	352	358	6	373	368
2.0×10^{-10}	364	375	12	392	380
9.7×10^{-12}	373	393	20	411	391
4.3×10^{-13}	382	411	29	430	401
2.2×10^{-14}	389	428	39	449	410
1.0×10^{-15}	396	446	51	468	418
5.1×10^{-17}	401	464	63	487	424
2.4×10^{-18}	405	481	77	506	429

[a]Ylisirniö et al.,[S2] [b]This study.

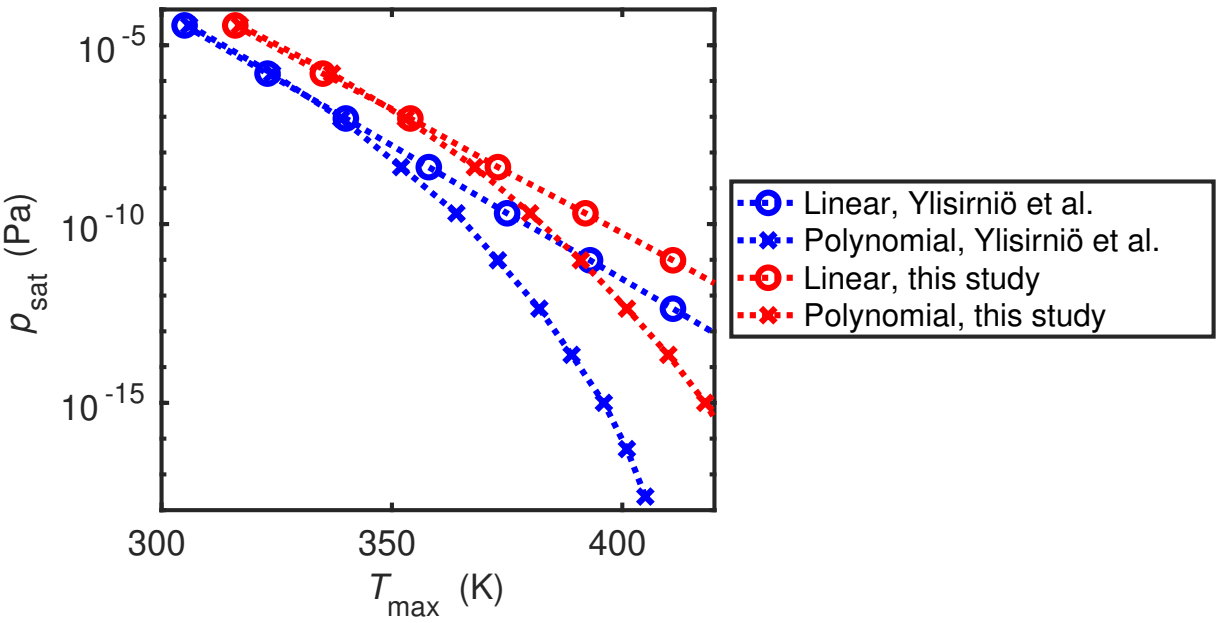

Figure S2: Different calibration curves shown in Table S2.

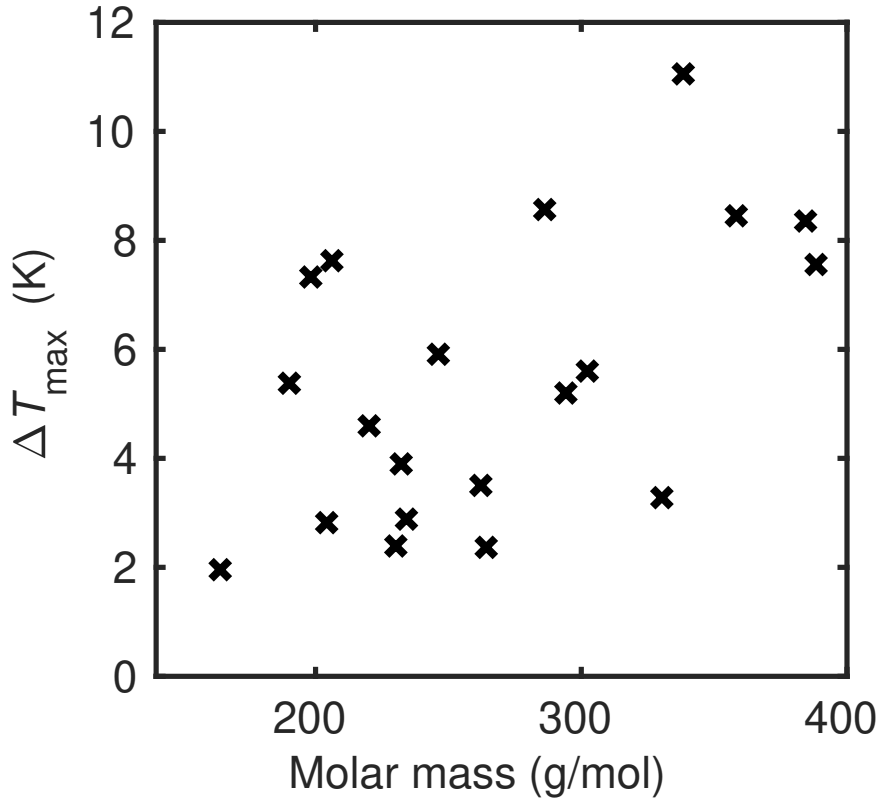

Figure S3: Difference between the highest and lowest $T_{\max}$ values in the 6 measurement cycles as a function of molar mass. Compounds thought to be products of thermal decomposition were not included.

S1 Conformer selection

To reduce the computational costs, we tested omitting conformers that contain intramolecular H-bonds already after the initial conformer sampling step. All distances between H-bond donors and acceptors were measured in Spartan14.[S3] We then removed all conformers that contained at least one donor–acceptor distance < 2.2 Å. Doing this, we were able to omit up to 98 % of the original conformers before starting density functional theory (DFT) calculations using TURBOMOLE.[S4] The reduction is significant especially in large monomers and dimers that have thousands of unique conformers.

In cases, where we did not find conformers containing no intramolecular H-bonds (after COSMO*conf* calculations), a new calculation was performed using the full set of conformers as input to COSMO*conf*. This way all conformers containing a single intramolecular H-bond are included in the initial conformer set.

Table S3 shows the number of conformers containing no intramolecular H-bonds we found using two initial conformer sets: one with all conformers found in systematic conformer search ("all") and the other with no conformers that contain intramolecular H-bonds ("0 H-bonds"). The same COSMO*conf* template was then used to optimize all conformers in the conformer sets and to remove duplicate conformers. With both initial conformer sets, COSMO*conf* produced a similar number of final conformers containing no intramolecular H-bonds. The largest difference in the saturation vapor pressure in our test calculations was a factor of 7.34, indicating that too many conformers were removed from the initial conformer set. For the other molecules, the small differences between the two conformer sets is caused by the removal of conformers with similar chemical potentials, in which different conformers were omitted depending on other conformers in the remaining conformer set.

Table S3: Comparison of saturation vapor pressures (p_{sat}) calculated using all conformers (all) or conformers containing no intramolecular H-bonds (0 H-bonds) as the input conformer set in COSMO*conf*.

	# 0 H-bond conformers		p_{sat} [Pa]		
	0 H-bonds	all	0 H-bonds	all	difference
$C_4H_4O_5$-iso2	5	6	1.06×10^{-1}	1.05×10^{-1}	1.01
$C_8H_{12}O_6$-iso4	7	8	7.68×10^{-6}	6.30×10^{-6}	1.22
$C_{10}H_{14}O_8$-iso2	18	15	1.03×10^{-6}	1.04×10^{-6}	0.99
Isomers from Kurtén et al.,[S5] calculated using the BP_TZVPD_FINE_19 parametrization					
$C_{10}H_{16}O_9$	> 40	> 40	6.63×10^{-8}	2.26×10^{-8} [b]	2.94
$C_{10}H_{16}O_{10}$	10	10	1.97×10^{-9}	1.97×10^{-9} [b]	1.00
$C_{20}H_{30}O_{10}$-iso1	> 40	> 40	1.29×10^{-10}	1.76×10^{-11} [b]	7.34
$C_{20}H_{30}O_{10}$-iso2	> 40	> 40	8.72×10^{-10}	8.74×10^{-10} [b]	1.00

[b] Hyttinen et al.[S6]

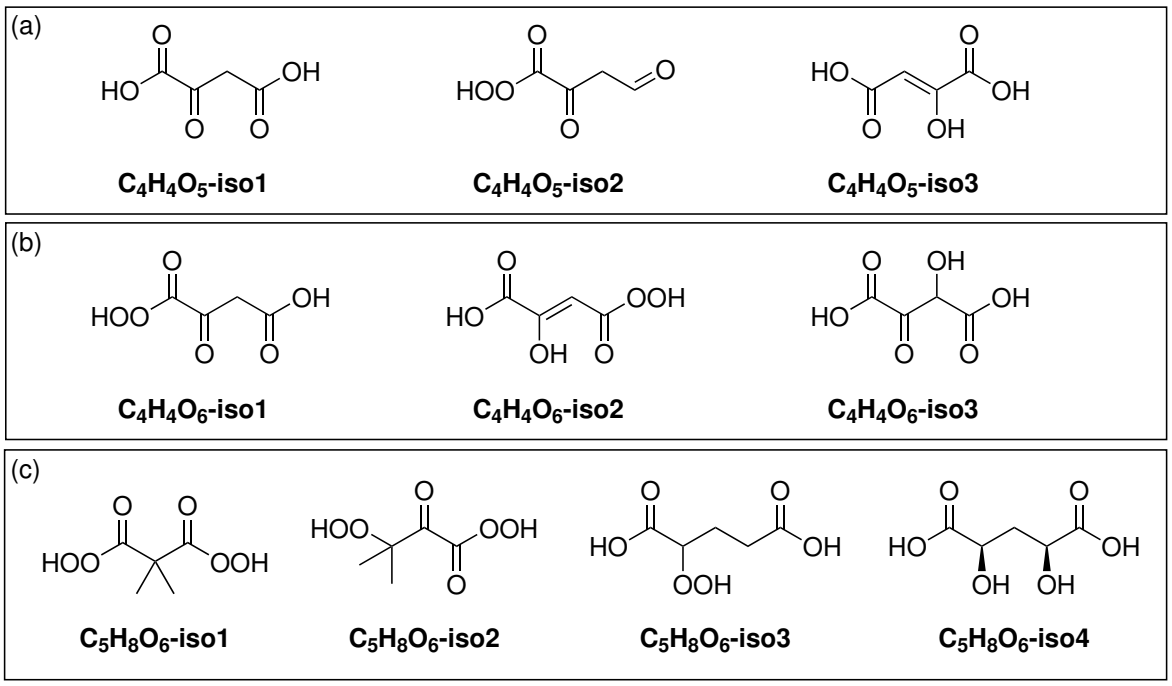

Figure S4: Structures of the studied (a) $C_4H_4O_5$, (b) $C_4H_4O_6$ and (c) $C_5H_8O_6$ isomers.

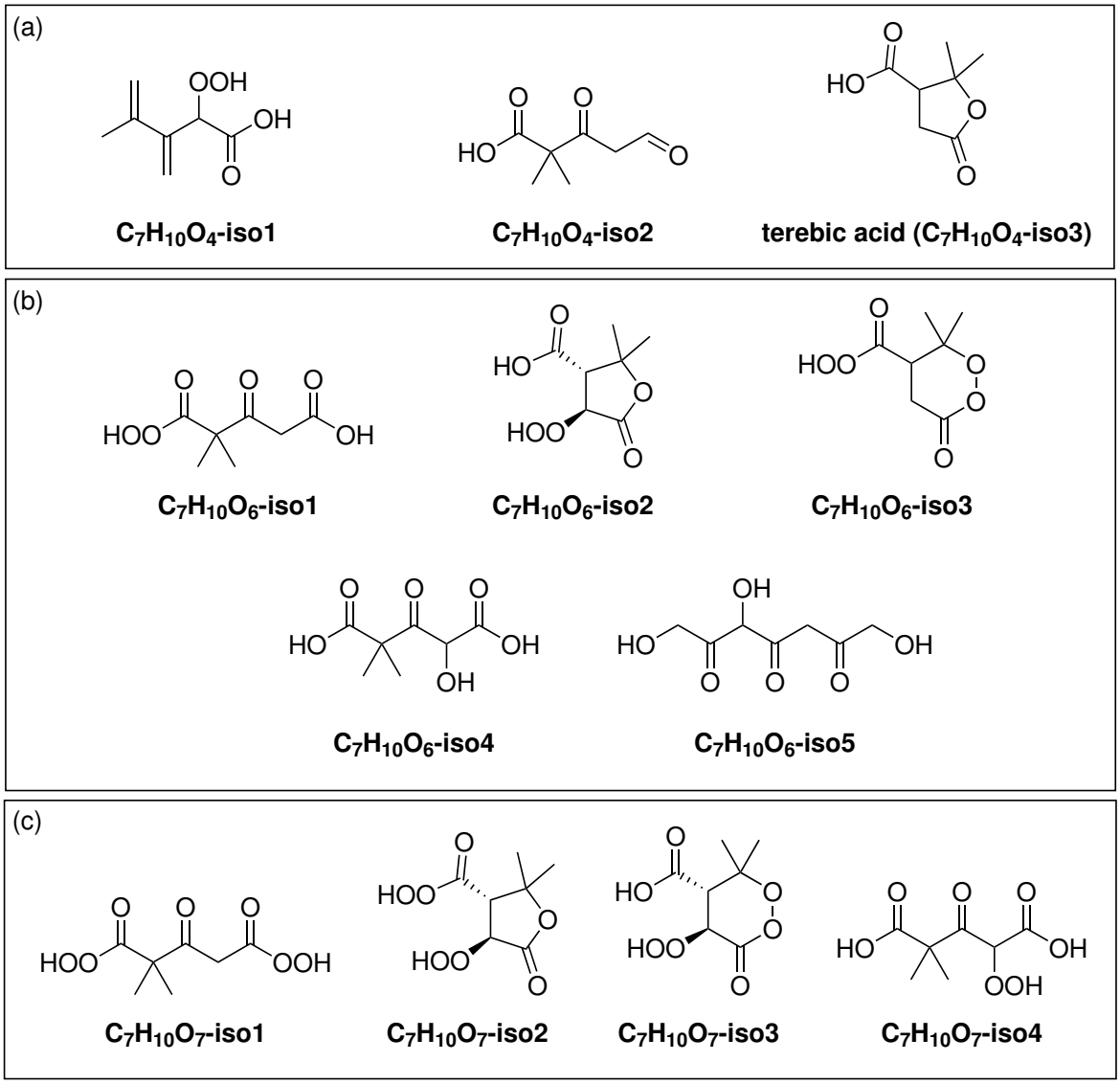

Figure S5: Structures of the studied (a) $C_7H_{10}O_4$, (b) $C_7H_{10}O_6$ and (c) $C_7H_{10}O_7$ isomers. Additional isomers for $C_7H_{10}O_4$ and $C_7H_{10}O_6$ are shown in Figures S11a and S11b, respectively, as products of thermal decomposition.

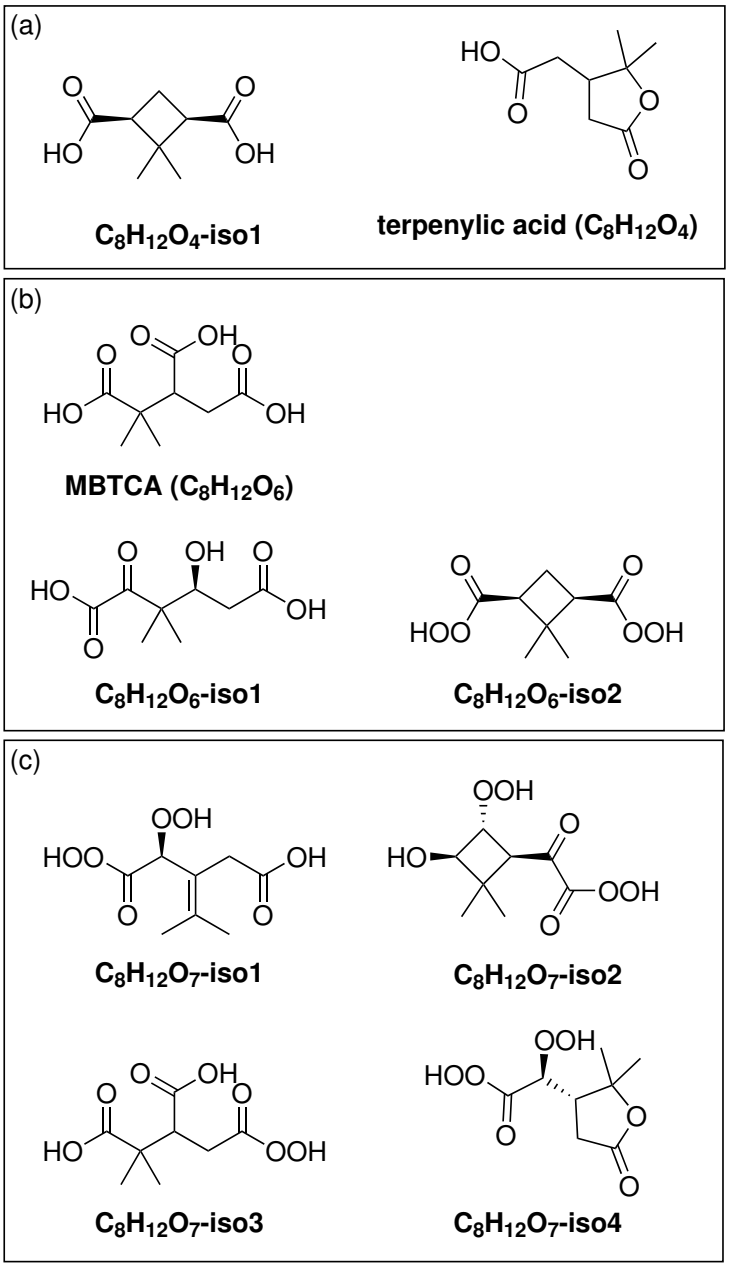

Figure S6: Structures of the studied (a) $C_8H_{12}O_4$, (b) $C_8H_{12}O_6$ and (c) $C_8H_{12}O_7$ isomers. Additional isomers for $C_8H_{12}O_4$ and $C_8H_{12}O_6$ are shown in Figures S12a and S12b, respectively, as products of thermal decomposition.

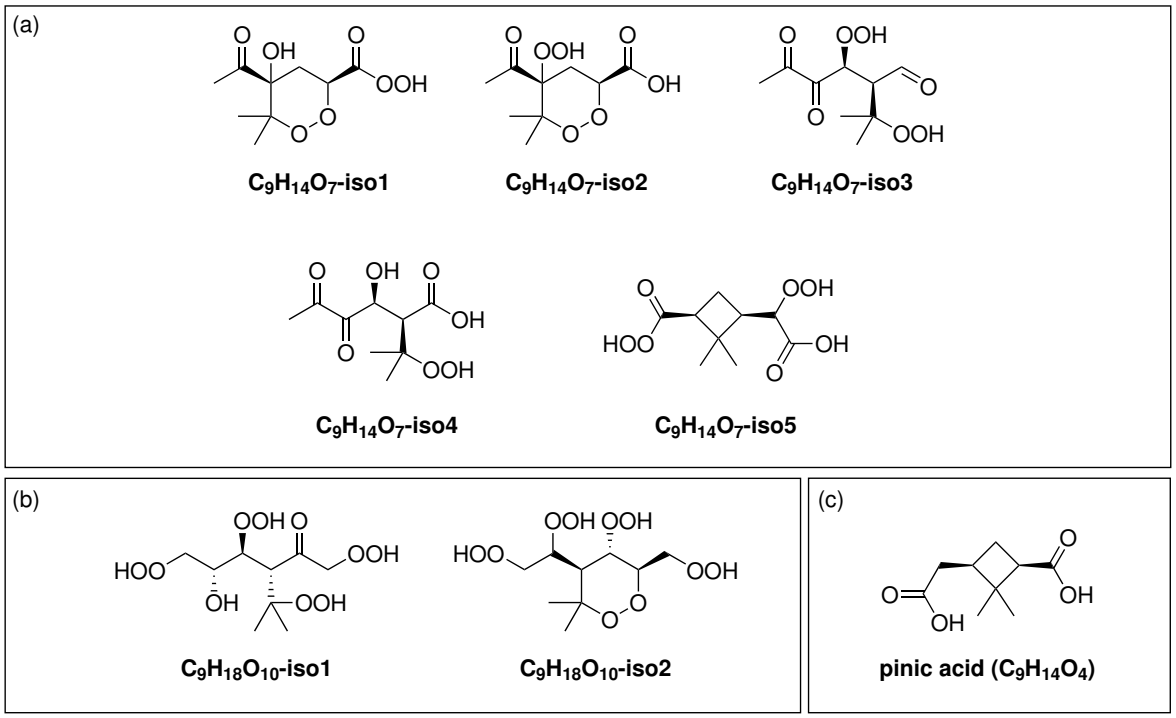

Figure S7: Structures of the studied (a) $C_9H_{14}O_7$, (b) $C_9H_{18}O_{10}$ and (c) $C_9H_{14}O_4$ isomers.

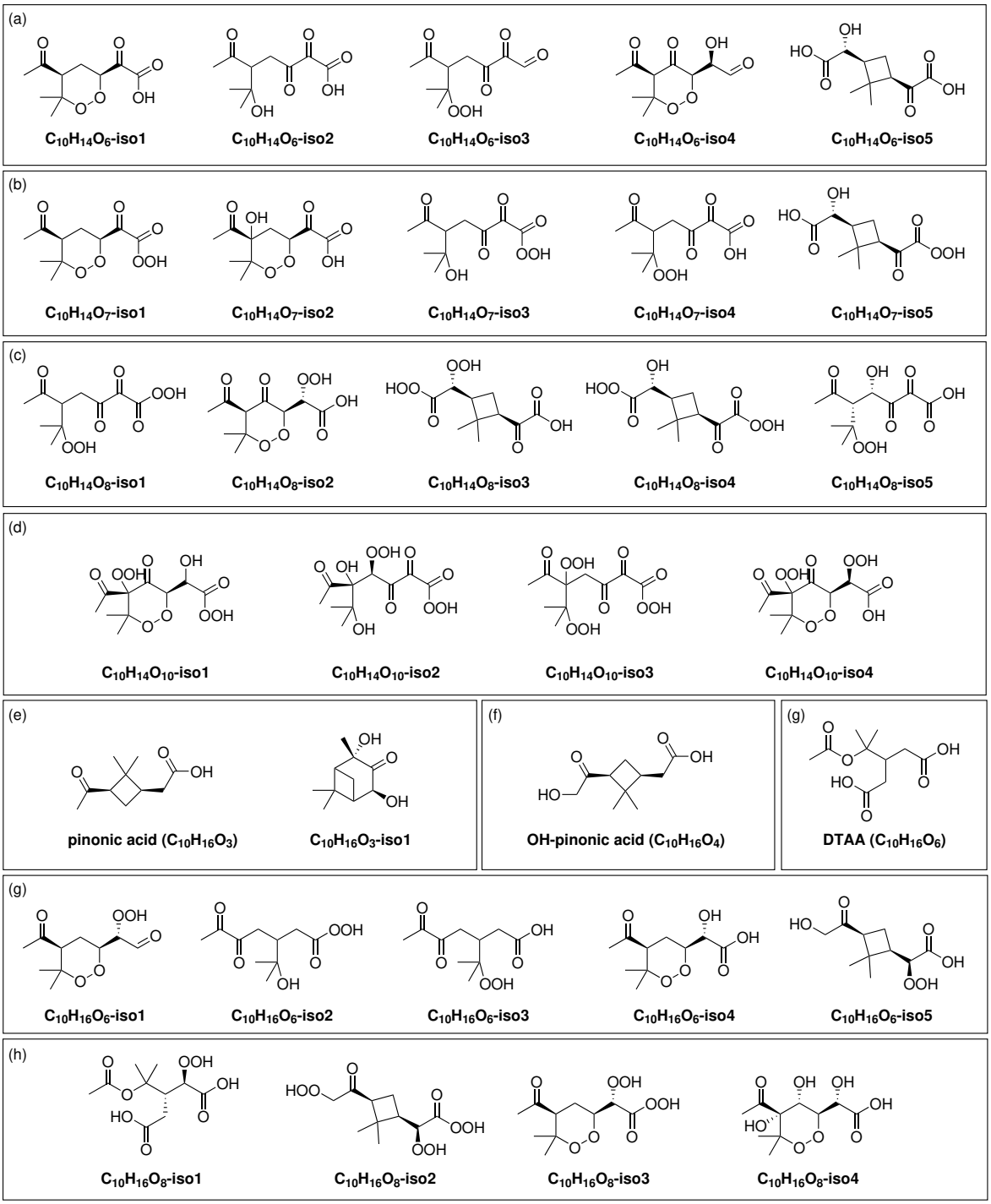

Figure S8: Structures of the studied (a) $C_{10}H_{14}O_6$, (b) $C_{10}H_{14}O_7$, (c) $C_{10}H_{14}O_8$, (d) $C_{10}H_{14}O_{10}$, (e) $C_{10}H_{16}O_3$, (f) $C_{10}H_{16}O_4$, (g) $C_{10}H_{16}O_6$ and (h) $C_{10}H_{16}O_8$ isomers.

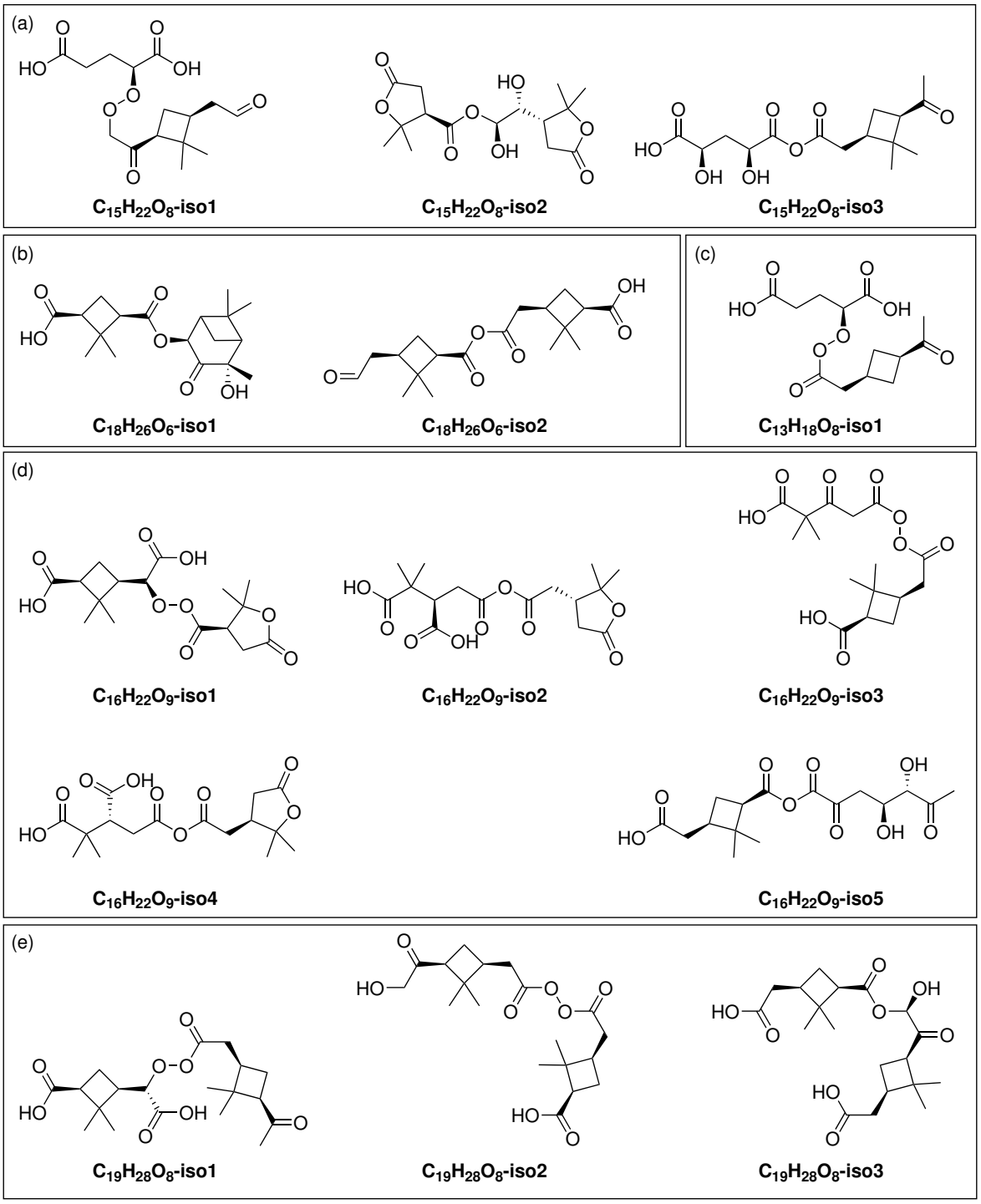

Figure S9: Structures of the studied (a) $C_{15}H_{22}O_8$, (b) $C_{18}H_{26}O_6$, (c) $C_{13}H_{18}O_8$, (d) $C_{16}H_{22}O_9$ and (e) $C_{19}H_{28}O_8$ dimer isomers.

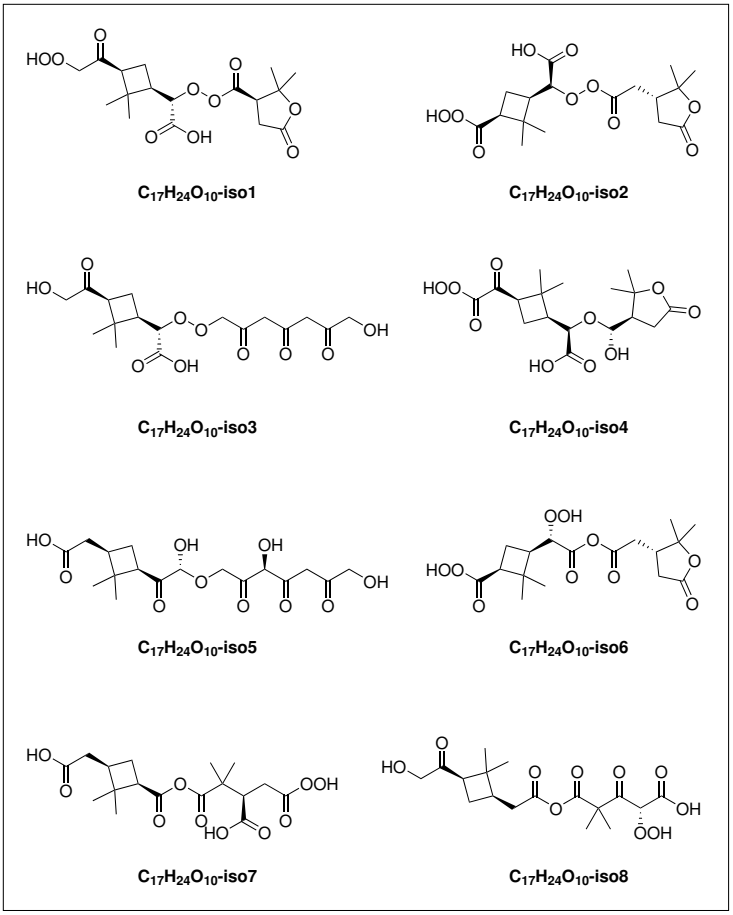

Figure S10: Structures of the studied $C_{17}H_{24}O_{10}$ dimer isomers.

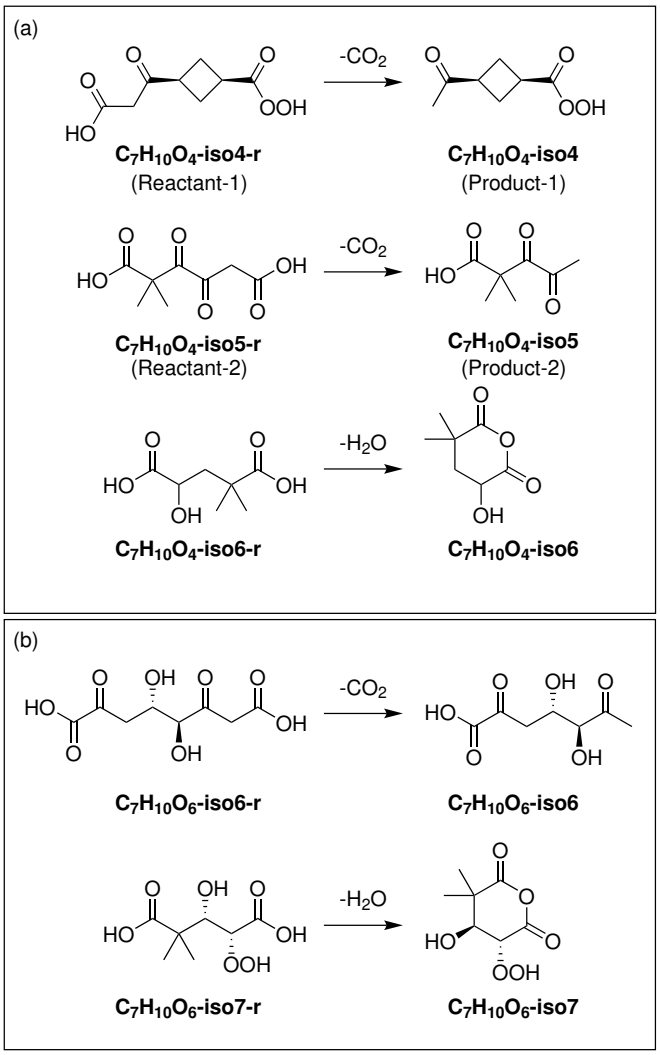

Figure S11: Structures of possible thermal decomposition products of (a) $C_7H_{10}O_4$ and (b) $C_7H_{10}O_6$, and the corresponding reactants of the decomposition reactions. Note that the reactants (labeled with "-r") have different elemental compositions than indicated by their names.

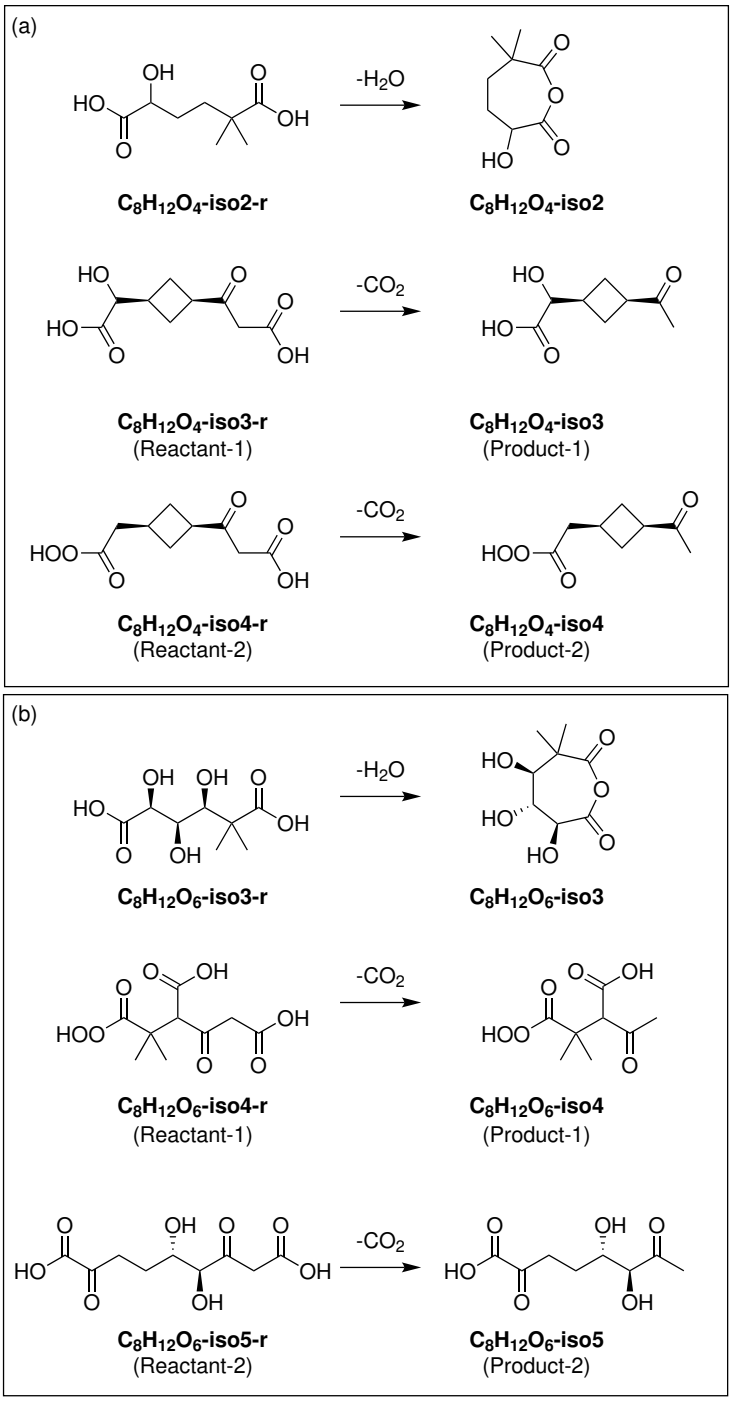

Figure S12: Structures of possible thermal decomposition products of (a) $C_8H_{12}O_4$ and (b) $C_8H_{12}O_6$, and the corresponding reactants of the decomposition reactions. Note that the reactants (labeled with "-r") have different elemental compositions than indicated by their names.

Table S4: Monomers that form the studied dimer isomers.

Monomers		Dimer
$C_5H_8O_6$ + $C_8H_{12}O_4$	$\xrightarrow{-2\,OH}$	$C_{13}H_{18}O_8$-iso1
$C_5H_8O_6$ + $C_{10}H_{16}O_4$	$\xrightarrow{-2\,OH}$	$C_{15}H_{22}O_8$-iso1
$C_7H_{10}O_4$ + $C_8H_{12}O_4$	$\rightarrow$	$C_{15}H_{22}O_8$-iso2
$C_5H_8O_6$ + $C_{10}H_{16}O_3$	$\xrightarrow{-H_2O}$	$C_{15}H_{22}O_8$-iso3
$C_8H_{12}O_4$ + $C_{10}H_{16}O_3$	$\xrightarrow{-H_2O}$	$C_{18}H_{26}O_6$-iso1
$C_9H_{14}O_4$ + $C_9H_{14}O_4$	$\xrightarrow{-2\,OH}$	$C_{18}H_{26}O_6$-iso2
$C_7H_{10}O_4$ + $C_9H_{14}O_7$	$\xrightarrow{-2\,OH}$	$C_{16}H_{22}O_9$-iso1
$C_8H_{12}O_4$ + $C_7H_{10}O_7$	$\xrightarrow{-2\,OH}$	$C_{16}H_{22}O_9$-iso2
$C_9H_{14}O_4$ + $C_7H_{10}O_7$	$\xrightarrow{-2\,OH}$	$C_{16}H_{22}O_9$-iso3
$C_8H_{12}O_4$ + $C_8H_{12}O_6$	$\xrightarrow{-H_2O}$	$C_{16}H_{22}O_9$-iso4
$C_9H_{14}O_4$ + $C_7H_{10}O_6$	$\xrightarrow{-H_2O}$	$C_{16}H_{22}O_9$-iso5
$C_{10}H_{16}O_3$ + $C_9H_{14}O_7$	$\xrightarrow{-2\,OH}$	$C_{19}H_{28}O_8$-iso1
$C_9H_{14}O_4$ + $C_{10}H_{16}O_6$	$\xrightarrow{-2\,OH}$	$C_{19}H_{28}O_8$-iso2
$C_9H_{14}O_4$ + $C_{10}H_{14}O_4$	$\rightarrow$	$C_{19}H_{28}O_8$-iso3
$C_7H_{10}O_4$ + $C_{10}H_{16}O_8$	$\xrightarrow{-2\,OH}$	$C_{17}H_{24}O_{10}$-iso1
$C_8H_{12}O_4$ + $C_9H_{14}O_8$	$\xrightarrow{-2\,OH}$	$C_{17}H_{24}O_{10}$-iso2
$C_7H_{10}O_6$ + $C_{10}H_{16}O_6$	$\xrightarrow{-2\,OH}$	$C_{17}H_{24}O_{10}$-iso3
$C_7H_{10}O_4$ + $C_{10}H_{14}O_6$	$\rightarrow$	$C_{17}H_{24}O_{10}$-iso4
$C_7H_{10}O_6$ + $C_{10}H_{14}O_4$	$\rightarrow$	$C_{17}H_{24}O_{10}$-iso5
$C_8H_{12}O_4$ + $C_9H_{14}O_7$	$\xrightarrow{-H_2O}$	$C_{17}H_{24}O_{10}$-iso6
$C_9H_{14}O_4$ + $C_8H_{12}O_7$	$\xrightarrow{-H_2O}$	$C_{17}H_{24}O_{10}$-iso7
$C_{10}H_{16}O_4$ + $C_7H_{10}O_7$	$\xrightarrow{-H_2O}$	$C_{17}H_{24}O_{10}$-iso8

Table S5: COSMO*therm*-estimated saturation vapor pressures (p_{sat}) and enthalpies of vaporization (ΔH_{vap}) of all studied monomers, dimers and reactants of thermal decomposition at 298.15 K.

Molecule name	Molar mass [g/mol]	p_{sat} [Pa]	ΔH_{vap} [kJ/mol]
Monomers			
$C_4H_4O_5$-iso1	132.07	6.64×10^{-2}	84.45
$C_4H_4O_5$-iso2	132.07	1.06×10^{-1}	83.11
$C_4H_4O_5$-iso3	132.07	3.02×10^{-2}	91.57
$C_4H_4O_6$-iso1	148.07	1.87×10^{-3}	101.47
$C_4H_4O_6$-iso2	148.07	5.47×10^{-3}	97.32
$C_4H_4O_6$-iso3	148.07	1.39×10^{-3}	102.18
$C_7H_{10}O_4$-iso1	158.15	1.32×10^{-2}	95.31
$C_7H_{10}O_4$-iso2	158.15	1.46×10^{-1}	83.55
terebic acid ($C_7H_{10}O_4$-iso3)	158.15	3.00×10^{-3}	93.99
$C_7H_{10}O_4$-iso4	158.15	1.55	68.17
$C_7H_{10}O_4$-iso5	158.15	6.54×10^{-1}	77.52
$C_7H_{10}O_4$-iso6	158.15	3.04×10^{-1}	79.24
$C_5H_8O_6$-iso1	164.11	1.58	71.20
$C_5H_8O_6$-iso2	164.11	2.29×10^{-2}	90.90
$C_5H_8O_6$-iso3	164.11	3.85×10^{-6}	127.28
$C_5H_8O_6$-iso4	164.11	2.86×10^{-7}	139.38
$C_8H_{12}O_4$-iso1	172.18	9.32×10^{-4}	104.54
$C_8H_{12}O_4$-iso2	172.18	1.23×10^{-2}	88.26
$C_8H_{12}O_4$-iso3	172.18	5.49×10^{-4}	102.45
$C_8H_{12}O_4$-iso4	172.18	1.84×10^{-3}	98.45
terpenylic acid ($C_8H_{12}O_4$)	172.18	1.72×10^{-4}	104.55
$C_{10}H_{16}O_3$-iso1	184.23	2.06×10^{-1}	87.00

Table S5 – continued from previous page

Molecule name	Molar mass [g/mol]	p_{sat} [Pa]	ΔH_{vap} [kJ/mol]
pinonic acid ($C_{10}H_{16}O_3$)	184.23	3.86×10^{-3}	95.55
$C_7H_{10}O_6$-iso1	190.15	1.40×10^{-4}	111.13
$C_7H_{10}O_6$-iso2	190.15	1.30×10^{-4}	110.73
$C_7H_{10}O_6$-iso3	190.15	3.19×10^{-2}	82.84
$C_7H_{10}O_6$-iso4	190.15	6.09×10^{-6}	124.93
$C_7H_{10}O_6$-iso5	190.15	1.27×10^{-7}	136.70
$C_7H_{10}O_6$-iso6	190.15	7.29×10^{-7}	132.58
$C_7H_{10}O_6$-iso7	190.15	6.05×10^{-3}	93.22
OH-pinonic acid ($C_{10}H_{16}O_4$)	200.23	1.01×10^{-5}	122.23
$C_8H_{12}O_6$-iso2	204.17	7.48×10^{-3}	92.88
$C_8H_{12}O_6$-iso3	204.17	5.48×10^{-6}	124.92
$C_8H_{12}O_6$-iso4	204.17	6.30×10^{-6}	120.62
MBTCA ($C_8H_{12}O_6$)	204.17	3.20×10^{-7}	138.42
$C_7H_{10}O_7$-iso1	206.15	1.83×10^{-6}	127.84
$C_7H_{10}O_7$-iso2	206.15	2.03×10^{-4}	108.90
$C_7H_{10}O_7$-iso3	206.15	6.97×10^{-3}	94.64
$C_7H_{10}O_7$-iso4	206.15	8.43×10^{-6}	125.11
$C_8H_{12}O_7$-iso1	220.17	2.65×10^{-8}	145.36
$C_8H_{12}O_7$-iso2	220.17	7.27×10^{-7}	137.07
$C_8H_{12}O_7$-iso3	220.17	8.30×10^{-8}	142.88
$C_8H_{12}O_7$-iso4	220.17	2.22×10^{-6}	127.22
$C_{10}H_{14}O_6$-iso1	230.21	2.47×10^{-6}	123.40
$C_{10}H_{14}O_6$-iso2	230.21	1.06×10^{-5}	122.16
$C_{10}H_{14}O_6$-iso3	230.21	1.65×10^{-4}	109.08

Table S5 – continued from previous page

Molecule name	Molar mass [g/mol]	p_{sat} [Pa]	ΔH_{vap} [kJ/mol]
$C_{10}H_{14}O_6$-iso4	230.21	6.12×10^{-3}	93.31
$C_{10}H_{14}O_6$-iso5	230.21	6.77×10^{-8}	142.53
$C_{10}H_{16}O_6$-iso1	232.23	4.79×10^{-5}	114.46
$C_{10}H_{16}O_6$-iso2	232.23	7.11×10^{-6} (3.6×10^{-2} [i])	125.84
$C_{10}H_{16}O_6$-iso3	232.23	1.24×10^{-5} (9.3×10^{-4} [i])	122.44
$C_{10}H_{16}O_6$-iso4	232.23	4.25×10^{-6}	126.26
$C_{10}H_{16}O_6$-iso5	232.23	7.38×10^{-9}	152.48
DTAA ($C_{10}H_{16}O_6$)	232.23	2.72×10^{-6}	128.78
$C_9H_{14}O_7$-iso1	234.20	3.68×10^{-7}	134.89
$C_9H_{14}O_7$-iso2	234.20	4.16×10^{-6}	126.52
$C_9H_{14}O_7$-iso3	234.20	1.16×10^{-5}	121.45
$C_9H_{14}O_7$-iso4	234.20	7.86×10^{-7}	134.75
$C_9H_{14}O_7$-iso5	234.20	3.21×10^{-8}	145.82
$C_{10}H_{14}O_7$-iso1	246.21	1.99×10^{-6}	127.51
$C_{10}H_{14}O_7$-iso2	246.21	4.14×10^{-7}	138.05
$C_{10}H_{14}O_7$-iso3	246.21	2.85×10^{-6}	127.50
$C_{10}H_{14}O_7$-iso4	246.21	2.28×10^{-6}	128.28
$C_{10}H_{14}O_7$-iso5	246.21	3.36×10^{-8}	148.67
$C_{10}H_{14}O_8$-iso1	262.21	6.29×10^{-7}	133.04
$C_{10}H_{14}O_8$-iso2	262.21	1.03×10^{-6}	132.94
$C_{10}H_{14}O_8$-iso3	262.21	4.60×10^{-8}	145.63
$C_{10}H_{14}O_8$-iso4	262.21	1.04×10^{-8}	150.49
$C_{10}H_{14}O_8$-iso5	262.21	2.69×10^{-8}	148.43

[i] Kurtén et al. [S5]

Table S5 – continued from previous page

Molecule name	Molar mass [g/mol]	p_{sat} [Pa]	ΔH_{vap} [kJ/mol]
$C_{10}H_{16}O_8$-iso1	264.22	4.32×10^{-8}	149.32
$C_{10}H_{16}O_8$-iso2	264.22	1.94×10^{-8}	149.88
$C_{10}H_{16}O_8$-iso3	264.22	1.62×10^{-7}	138.41
$C_{10}H_{16}O_8$-iso4	264.22	4.46×10^{-8}	148.82
$C_9H_{18}O_{10}$-iso1	286.23	1.64×10^{-11}	182.20
$C_9H_{18}O_{10}$-iso2	286.23	2.43×10^{-9}	159.49
$C_{10}H_{14}O_{10}$-iso1	294.21	1.63×10^{-10}	167.55
$C_{10}H_{14}O_{10}$-iso2	294.21	1.81×10^{-8}	151.20
$C_{10}H_{14}O_{10}$-iso3	294.21	1.19×10^{-8}	152.74
$C_{10}H_{14}O_{10}$-iso4	294.21	1.29×10^{-9}	159.26
Thermal decomposition reactants			
$C_7H_{10}O_4$-iso4-r	202.16	5.47×10^{-7}	129.96
$C_7H_{10}O_4$-iso5-r	202.16	1.74×10^{-4}	113.21
$C_7H_{10}O_4$-iso6-r	176.16	2.70×10^{-5}	121.40
$C_8H_{12}O_4$-iso2-r	190.19	5.54×10^{-6}	128.99
$C_8H_{12}O_4$-iso3-r	216.18	2.28×10^{-9}	154.76
$C_8H_{12}O_4$-iso4-r	216.18	3.32×10^{-7}	134.07
$C_7H_{10}O_6$-iso6-r	234.16	2.52×10^{-11}	169.09
$C_7H_{10}O_6$-iso7-r	208.16	5.40×10^{-8}	146.36
$C_8H_{12}O_6$-iso3-r	222.19	1.40×10^{-11}	177.75
$C_8H_{12}O_6$-iso4-r	248.18	3.28×10^{-11}	169.43
No experimental p_{sat}			
pinic acid ($C_9H_{14}O_4$)	186.20	2.57×10^{-4}	109.58
Dimers			

Table S5 – continued from previous page

Molecule name	Molar mass [g/mol]	p_{sat} [Pa]	ΔH_{vap} [kJ/mol]
$C_{13}H_{18}O_8$-iso1	302.27	1.87×10^{-10}	167.55
$C_{15}H_{22}O_8$-iso1	330.32	2.06×10^{-11}	175.86
$C_{15}H_{22}O_8$-iso2	330.32	1.27×10^{-12}	181.47
$C_{15}H_{22}O_8$-iso3	330.32	2.42×10^{-11}	178.93
$C_{16}H_{22}O_9$-iso1	358.33	9.15×10^{-12}	180.50
$C_{16}H_{22}O_9$-iso2	358.33	4.32×10^{-13}	192.59
$C_{16}H_{22}O_9$-iso3	358.33	1.10×10^{-9}	166.08
$C_{16}H_{22}O_9$-iso4	358.33	5.03×10^{-13}	191.80
$C_{16}H_{22}O_9$-iso5	358.33	9.20×10^{-12}	185.72
$C_{17}H_{24}O_{10}$-iso1	388.36	3.12×10^{-13}	190.29
$C_{17}H_{24}O_{10}$-iso2	388.36	3.96×10^{-14}	200.56
$C_{17}H_{24}O_{10}$-iso3	388.36	4.25×10^{-14}	208.97
$C_{17}H_{24}O_{10}$-iso4	388.36	3.93×10^{-15}	210.91
$C_{17}H_{24}O_{10}$-iso5	388.36	2.17×10^{-14}	213.43
$C_{17}H_{24}O_{10}$-iso6	388.36	5.27×10^{-13}	190.36
$C_{17}H_{24}O_{10}$-iso7	388.36	5.77×10^{-13}	194.38
$C_{17}H_{24}O_{10}$-iso8	388.36	8.56×10^{-13}	195.08
$C_{18}H_{26}O_6$-iso1	338.39	4.08×10^{-7}	141.43
$C_{18}H_{26}O_6$-iso2	338.39	1.19×10^{-7}	140.03
$C_{19}H_{28}O_8$-iso1	384.41	5.14×10^{-12}	186.15
$C_{19}H_{28}O_8$-iso2	384.41	2.17×10^{-10}	174.36
$C_{19}H_{28}O_8$-iso3	384.41	3.26×10^{-12}	189.87

Table S6: Experimental $T_{\max}$ values from 6 subsequent thermal desorptions in Kelvin.

compound	cycle 2	cycle 3	cycle 4	cycle 5	cycle 6	cycle 7
$C_4H_4O_5$	343.74	348.67	346.32	351.78	345.86	354.61
$C_4H_4O_6$	448.78	449.11	448.40	447.60	447.66	442.00
$C_7H_{10}O_4$	344.74	346.32	346.32	348.36	348.18	348.97
$C_5H_8O_6$	350.75	351.33	351.33	352.49	352.30	352.71
$C_9H_{12}O_3$	444.53	444.26	446.58	438.11	441.76	-
$C_8H_{12}O_4$	350.45	353.98	352.82	352.49	351.98	355.35
$C_{10}H_{16}O_3$	327.84	325.69	327.82	325.16	326.01	325.00
$C_9H_{14}O_4$	348.30	344.93	344.93	346.53	-	-
$C_7H_{10}O_6$	346.64	350.17	350.03	351.98	348.66	352.02
$C_{10}H_{14}O_4$	388.44	393.09	393.09	394.35	391.85	387.02
$C_8H_{12}O_6$	357.10	358.71	358.71	359.92	359.75	359.76
$C_7H_{10}O_7$	353.35	354.00	354.00	356.04	348.41	354.77
$C_8H_{12}O_7$	346.64	349.08	350.58	348.36	350.36	351.24
$C_{10}H_{14}O_6$	358.33	357.11	357.06	356.04	355.94	356.66
$C_{10}H_{16}O_6$	335.45	335.05	335.84	336.12	333.00	332.22
$C_9H_{14}O_7$	358.33	357.74	360.61	360.62	359.56	360.31
$C_{10}H_{14}O_7$	350.45	353.60	353.98	355.68	355.36	356.36
$C_{10}H_{14}O_8$	350.45	350.17	350.17	352.49	352.70	353.67
$C_{10}H_{16}O_8$	362.06	363.58	364.43	363.97	362.50	362.81
$C_9H_{18}O_{10}$	370.09	375.04	375.04	375.90	372.43	378.66
$C_{10}H_{14}O_{10}$	362.86	365.65	365.92	368.06	364.73	364.16
$C_{13}H_{18}O_8$	390.00	391.69	391.69	392.00	388.10	386.40
$C_{15}H_{22}O_8$	383.11	385.54	385.05	383.94	383.30	382.26
$C_{18}H_{26}O_6$	363.16	365.96	368.19	374.22	368.89	371.33
$C_{16}H_{22}O_9$	393.99	393.61	393.61	395.00	392.30	386.55
$C_{19}H_{28}O_8$	377.94	386.30	385.54	380.06	381.45	-
$C_{17}H_{24}O_{10}$	390.00	397.56	394.53	-	-	-
$C_{20}H_{34}O_{10}$	379.96	385.54	385.54	383.94	387.95	382.36

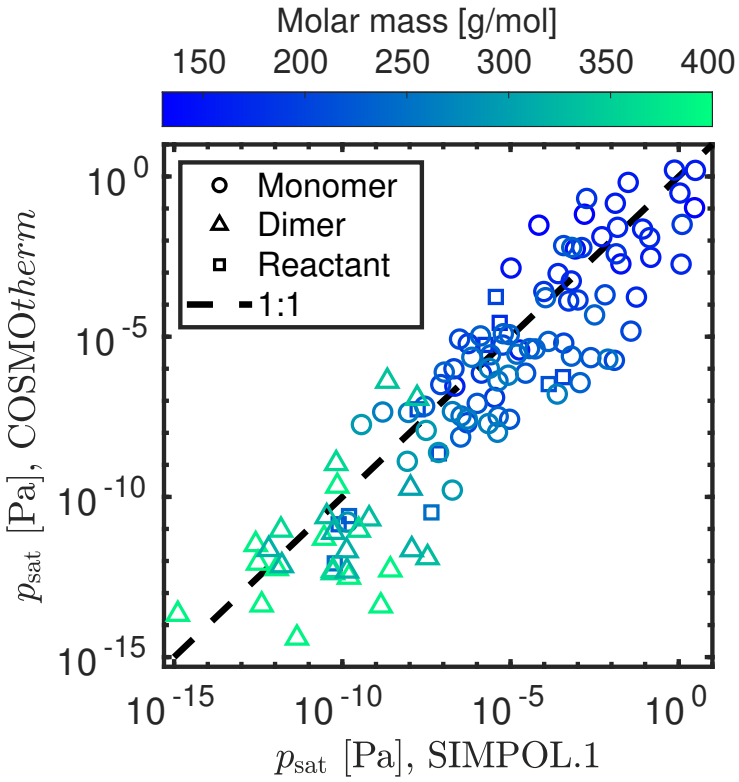

Figure S13: Saturation vapor pressures of all studied monomers, dimers and thermal decomposition reactants estimated using COSMO*therm* and SIMPOL.1 at 298.15K.

S2 The effect of dimer formation on COSMO*therm* saturation vapor pressures

The size-dependence of S in equation 4 was tested using polyethylene glycol (PEG; $H(OC_2H_4)_mOH$) molecules with m=2–8 (see Figure S14). We see that S is clearly higher when the p_{sat} value of the PEG is estimated using PEG1 than using only PEG2–PEG7. This result is likely caused by the relatively low COSMO*therm*-estimated p_{sat} of PEG1 (if a logarithmic size dependence is assumed for the p_{sat} of the PEG series). No clear correlation is seen between S and the monomer size (PEG or α-pinene-derived monomers) with the exception of PEG1 (see Figure S14). The SIMPOL.1 group-contribution method predicts $S = 6.5\times10^{-4}$ for all PEG dimerization reactions.

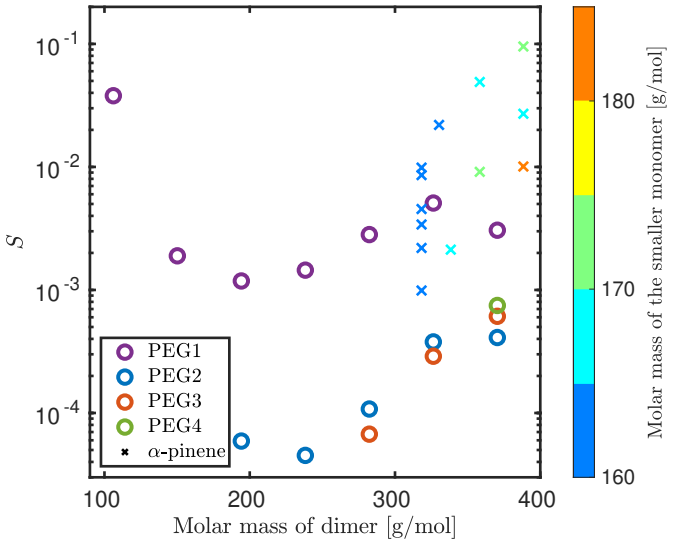

Figure S14: Molar mass dependence of S in COSMO*therm*-derived saturation vapor pressures of polyethylene glycols (PEG2-PEG8) and α-pinene-derived acid anhydride dimers. The colors indicate the size of the smaller monomer used to form the dimer. E.g., PEG8 can be formed from dimerization of PEG1 and PEG7, PEG2 and PEG6, PEG3 and PEG5, or two PEG4 molecules, giving four different values of S.

References

(S1) Krieger, U. K.; Siegrist, F.; Marcolli, C.; Emanuelsson, E. U.; Gøbel, F. M.; Bilde, M.; Marsh, A.; Reid, J. P.; Huisman, A. J.; Riipinen, I.; Hyttinen, N.; Myllys, N.; Kurtén, T.; Bannan, T.; Percival, C. J.; Topping, D. A reference data set for validating vapor pressure measurement techniques: homologous series of polyethylene glycols. *Atmos. Meas. Tech.* **2018**, *11*, 49–63.

(S2) Ylisirniö, A.; Barreira, L. M. F.; Pullinen, I.; Buchholz, A.; Jayne, J.; Krechmer, J. E.; Worsnop, D. R.; Virtanen, A.; Schobesberger, S. On the calibration of FIGAERO-ToF-CIMS: importance and impact of calibrant delivery for the particle-phase calibration. *Atmos. Meas. Tech.* **2021**, *14*, 355–367.

(S3) Spartan'14, Wavefunction Inc., Irvine, CA. 2014.

(S4) TURBOMOLE, a development of University of Karlsruhe and Forschungszentrum Karlsruhe GmbH, TURBOMOLE GmbH, Version 7.4.1. 2010.

(S5) Kurtén, T.; Tiusanen, K.; Roldin, P.; Rissanen, M.; Luy, J.-N.; Boy, M.; Ehn, M.; Donahue, N. α-Pinene autoxidation products may not have extremely low saturation vapor pressures despite high O:C ratios. *J. Phys. Chem. A* **2016**, *120*, 2569–2582.

(S6) Hyttinen, N.; Wolf, M.; Rissanen, M. P.; Ehn, M.; Peräkylä, O.; Kurtén, T.; Prisle, N. L. Gas-to-Particle Partitioning of Cyclohexene- and α-Pinene-Derived Highly Oxygenated Dimers Evaluated Using COSMO*therm*. *J. Phys. Chem. A* **2021**, *125*, 3726–3738.